Journal of Solid State Chemistry **142,** 273–278 (1999)
Article ID jssc.1998.7983, available online at http://www.idealibrary.com on IDEAL®

Electron Density Study of Garnets: $Z_3Al_2Si_3O_{12}$ (Z = Mg, Fe, Mn, Ca) and $Ca_3Fe_2Si_3O_{12}$

Haruo Sawada

Department of Applied Chemistry, Kogakuin University, 2665-1 Nakano-machi, Hachioji, Tokyo 192-0015, Japan

Received March 24, 1998, accepted July 15, 1998

The crystal structures of seven crystals from five garnet mineral species have been studied through single-crystal X-ray diffraction methods incorporating scattering factor refinement procedures. The derived experimental scattering factors for each atomic species show similar scattering-angle-dependent patterns in their deviations from the theoretical factors. The Si–O distances remain virtually unchanged in the Ca garnets even though the cell constants and the other cation–oxygen distances change with composition. Electron density residuals indicating bonding electrons are seen in all seven crystals, with ~ 0.2 e/Å^3 height between Si and oxygen. Two crystals containing divalent Fe show a characteristic electron density deformation indicating the orientation of the *d* orbital with paired electrons. © 1999 Academic Press

INTRODUCTION

A generic formula $Z_3X_2T_3O_{12}$ is used for generally notating the 8-fold (Z), 6-fold (X), and 4-fold [T (= Si in the present work)] coordinated cation sites in garnets (Wyckoff positions 24*c*, 16*a*, and 24*d*, respectively).

A recent study on four rare-earth Ga garnets (1) has shown the various trends of the experimentally derived scattering factors; in all cases, oxygen and Ga exhibited smaller than theoretical scattering factor values at low scattering angles ($\sin\theta/\lambda < 0.4$) but settled close to the theoretical values at higher angles. The Z site, accommodating the rare-earth ions, showed a variety of electron density deformation from spherical, indicating the various modes in the occupation of the f orbitals. Electron density residuals around the X site due to the d electrons of Cr^{3+} were seen in another garnet, $Ca_3(Cr,Al)_2Si_3O_{12}$ (2).

In the present work, the crystal structures of seven silicate garnets are refined with mostly the same techniques used in these previous studies. A survey of the structural aspects of natural silicate garnets can be found in a previous study (3). Oxygen and Si constitute the O and T sites, respectively, for all seven crystals; six samples have Al at the X site, and three have Ca at the Z site. General tendencies of the scattering factors unique to each of these atomic species are expected to become evident.

EXPERIMENTAL

The abbreviations used and the chemical compositions analyzed with an electron microprobe (JSM-5400S electron microscope equipped with a LINK-QV2000 energy-dispersive X-ray detector) are listed in Table 1; various conditions for experiment and structure refinement are given in Table 2. All crystals used in the X-ray diffraction experiments were rounded into spheres.

Cell dimensions were determined from the setting angles of the 24 equivalents of the 16,16,8 reflection (Rigaku AFC5 automated four-circle diffractometer (40 kV, 30 mA), graphite-monochromated Mo$K\alpha_1$ radiation (0.70926 Å)). Intensity data were collected with Mo$K\alpha$ radiation (0.7017 Å) with the 2θ–ω scan. Equivalent reflections were generated from initially measured independent reflections observed with $|F_o| > 6\sigma(F_o)$ (Table 2). Those with all additionally measured equivalents observed with $|F_o| > 6\sigma(F_o)$ were averaged into the finally used number of independent data.

The crystal structure was refined with a modified version of the program RADY (4), applying Lp, absorption, and isotropic extinction corrections, using fully ionized scattering factors (5, 6) and dispersion correction values (7). Weights proportional to the theoretical number of equivalents for each reflection were allotted.

The experimental scattering factors for each structure were derived through procedures identical to those in previous studies (1, 2). Anharmonic refinement with Gram–Charlier series-expanded parameters up to the sixth-rank tensors (symmetry restrictions taken from (8)) was run next.

DISCUSSION

The experimentally obtained scattering-angle-dependent spherical scattering factors show similarities within each atomic species (Fig. 1). The trend seen in oxygen, showing scattering factors smaller than the theoretical factors at low $\sin\theta/\lambda$ ranges, is commonly observed in most of the oxides

0022-4596/99 $30.00

TABLE 1
Mineral Species, Abbreviations Used, Compositions Used in Calculating the Theoretical Scattering Factors of Each Site and Origin of the Garnet Crystals[a]

Pyrope	MgAG	$Mg_3Al_2Si_3O_{12}$[b]	Cuneo, Italy
Almandine	FAG	$(Fe_{2.25}Mg_{0.42}Mn_{0.26}Ca_{0.08})(Al_{1.96}Fe_{0.04})Si_3O_{12}$	Mataramaki, Finland
Spessartine	MnAG#1	$(Mn_{2.21}Fe_{0.79})Al_2Si_3O_{12}$	Nagano, Japan
Spessartine	MnAG#2	$(Mn_{2.37}Ca_{0.63})Al_2Si_3O_{12}$	Kyoto, Japan
Grossular	CAG#1, CAG#2	$Ca_3Al_2Si_3O_{12}$[b]	Quebec, Canada
Andradite	CFG	$Ca_3Fe_2Si_3O_{12}$[b]	Arizona, U.S.A.
Uvarovite[c]	CCG	$Ca_3(Cr_{1.10}Al_{0.80}Ti_{0.06}Fe_{0.03})Si_3O_{12}$	Ural Mountains, Russia

Note. Since the microprobe analyses (oxygen was not analyzed) showed no indication of substitution for Si, the full values Si_3 and O_{12} were assumed for the T and O sites.

[a]Derived from occupancy refinement except for FAG and CCG, where the analyzed composition was used,

[b]Pure to within 1 at.% for each site in the microprobe analyses. Assumed pure in the structure refinement.

[c]Reference (2).

studied so far (such as in (1), (2), and (9–11)). The patterns for Si and those for Al show mutual resemblance and, along with Mg at the Z site in MgAG, show larger than theoretical values at low $\sin\theta/\lambda$ ranges. Similar trends can be seen for Al or Mg in several other compounds (12–14). Ca in the Z site does not seem to deviate much from theoretical values.

The Si–O distances show expansion with the increase of the cell constants for garnets with smaller cells; however, for

TABLE 2
Experimental and Structure Refinement Conditions

	MgAG	FAG	MnAG#1	MnAG#2	CAG#1	CAG#2	CFG
Crystal diameter (mm)	0.25	0.20	0.24	0.28	0.39	0.25	0.30
2θ value of 16, 16, 8 (deg)	95.94	95.09	94.44	93.87	91.81	91.81[a]	89.78
a (Å)	11.4582 (5)	11.5357 (6)	11.596 (14)	11.6501 (7)	11.8504 (4)	11.8504 (4)[a]	12.0602 (10)
D_x (g/cm^3)	3.560	4.190	4.223	4.159	3.596	3.596[a]	3.849
F (000)	1600	1887	1918	1912	1792	1792[a]	2000
μ (cm^{-1})	11.77	55.37	56.01	52.88	26.56	26.56[a]	55.06
Scan width: $a + b \tan\theta$ in ω (deg)							
a	1.8	1.75	1.85	1.9	1.75	1.85	2.0
b	0.35	0.15	0.25	0.25	0.25	0.3	0.2
Scan speed (min^{-1}) in ω (deg)	16	10	16	16	16	6	16
Maximum number of repeats	10	10	10	10	3	3	3
Repeated until: $\lvert F_o\rvert/\sigma(F_o) >$	10.0	10.0	10.0	10.0	10.0	100.0	10.0
Maximum 2θ (deg)	140.0	140.0	140.0	140.0	140.0	120.	140.0
Maximum index	30	30	30	30	31	28	31
Initially measured independents							
Measured	1209	1335	1350	1370	1366	1064	1429
Observed	660	554	640	572	717	564	476
Initially observed (+)							
Generated equivalents	4521[b]	3165[b]	4686[b]	4553[b]	13587	1957	8418
Used to average	3283	2929	3210	2668	11273	1707	6896
Used independent data	554	492	537	448	556[c]	461	369
R_{int}	0.0116	0.0107	0.0116	0.0139	0.0068	0.0108	0.0066
Reciprocal space covered for hkl reflections	1/8	1/8	1/8	1/8	1/2	1/12	1/2
Harmonic refinement							
Number of scattering factor refinement iterations	10	12	4	21	5	6	13
R	0.0126	0.0128	0.0132	0.0129	0.0080	0.0122	0.0067
R_w	0.0130	0.0126	0.0140	0.0135	0.0088	0.0125	0.0076
Anharmonic refinement							
Number of scattering factor refinement iterations	2	0	0	0	37	2	22
R	0.0111	0.0107	0.0115	0.0109	0.0072	0.0099	0.0055
R_w	0.0113	0.0106	0.0123	0.0112	0.0077	0.0102	0.0061

[a]The value for CAG#1 was used.

[b]Seven additional equivalents were generated for hhh reflections, five for the other types.

[c]Eight reflections (400, 420, 444, 640, 642, 800, 880, and 888) were omitted since there were effects believed to be due to having uncorrectably strong secondary extinction registering $F_o < 0.8F_c$ even after corrections. The 220 reflection, which had a large scatter in F_o values among the eqauivalents, was also omitted.

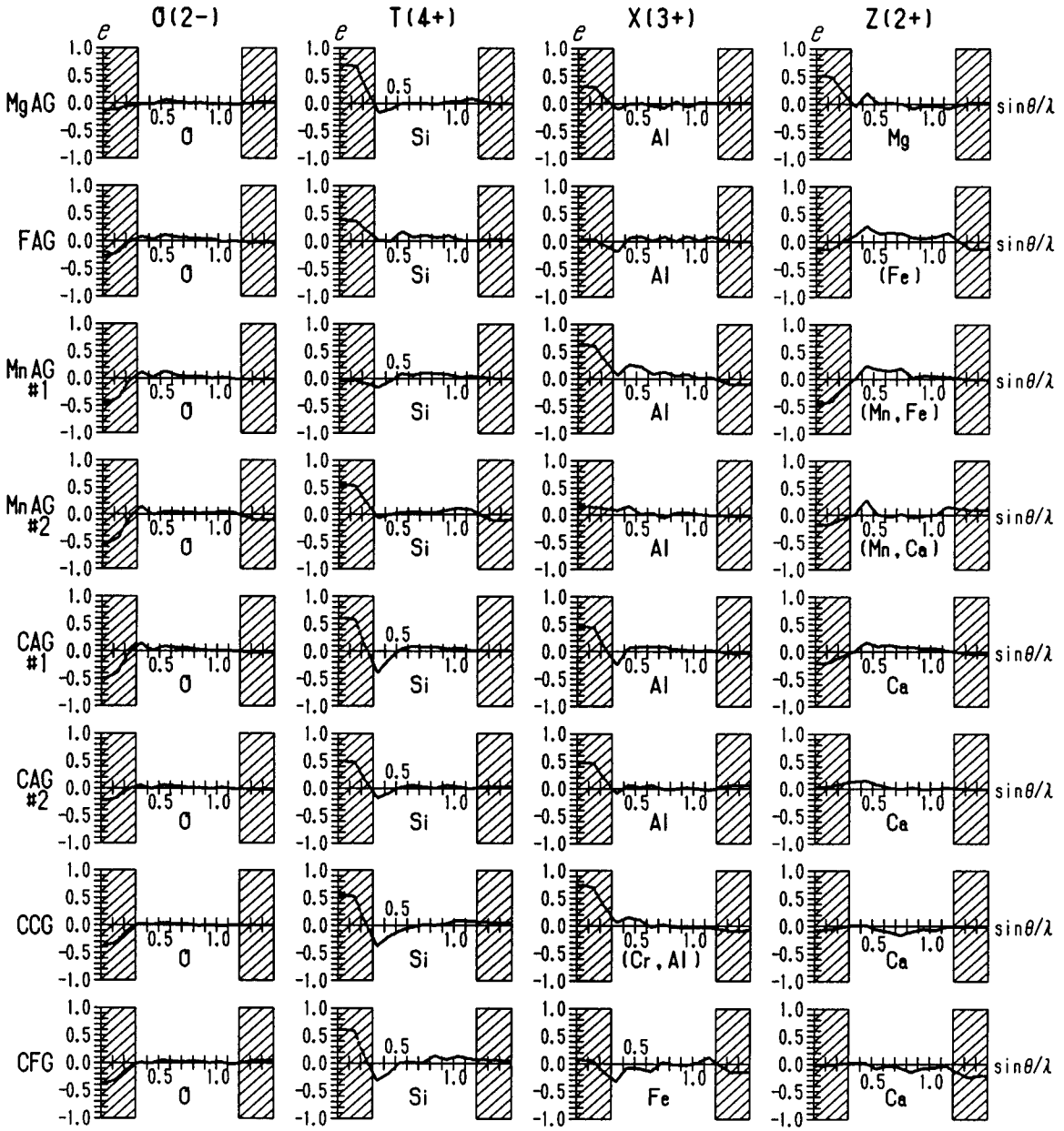

FIG. 1. Scattering factors derived from scattering factor refinement with the harmonic parameters subtracted by the theoretical values. The $\sin\theta/\lambda$ range outside the fully interpolated region is shown hatched. The plot for CCG (Ref. (2); Table 1) is also shown.

the Ca garnets, the distances are practically unchanged (Table 3). In these garnets, ~ 1.647 Å seems to be the upper limit for the Si–O distance. The X–O and Ca–O distances expand with increase of the cell constants.

Electron density residuals corresponding to covalent bonding-type electrons are seen (Fig. 2) with an average of approximately 0.2 e/Å^3 height between Si and oxygen, and weak positive regions of ~ 0.1 e/Å^3 height in the Al–O bonding directions in MgAG and FAG, which have the closest Al–O distances in the currently studied compounds and which can be considered to have the most covalency. The latter feature was also seen in α-Al_2O_3 (14), $MgAl_2O_4$ (15), and $Y_3Al_5O_{12}$ (12).

The Fe^{2+} garnets show a conspicuous electron density deformation (Fig. 3) at the Z site. Divalent Fe has six d electrons, one each in the five orbitals plus one. The oxygen coordination of the Z site can be considered to be distorted cubic; thus the sixth electron enters the orbital which, in an ideal cubic field, corresponds to the e_g type. The sites show clearly the large electron density residuals corresponding to the (+) symmetry lobes, accompanied by the doughnut-shaped (−) symmetry region encircling the equator, thus

TABLE 3
Variable Positional Parameters for Oxygen in Fractional Coordinates, Equivalent Isotropic Factors $B = (8\pi^2/3)(\sum\sum U_{ij} a_i^* a_j^* a_i \cdot a_j)$ (Å^2), and Nearest Cation–Anion Disances (Å)[a]

	MgAG	FAG	MnAG#1	MnAG#2	CAG#1	CAG#2	CCG	CFG
				Harmonic refinement				
O								
x	0.03301(3)	0.03406(4)	0.03476(4)	0.03532(5)	0.03825(2)	0.03828(2)	0.03893(3)	0.03938(4)
y	0.05024(3)	0.04893(4)	0.04834(4)	0.04732(5)	0.04523(2)	0.04531(4)	0.04676(3)	0.04850(4)
z	0.65329(3)	0.65287(4)	0.65267(4)	0.65232(5)	0.65131(2)	0.65138(4)	0.65322(3)	0.65530(4)
B								
O	0.488	0.455	0.462	0.518	0.367	0.391	0.443	0.450
T	0.295	0.283	0.301	0.348	0.246	0.277	0.331	0.331
X	0.312	0.356	0.233	0.337	0.285	0.311	0.257	0.364
Z	0.652	0.586	0.592	0.628	0.384	0.404	0.429	0.445
T–O	1.6341(3)	1.6354(5)	1.6380(5)	1.6402(6)	1.6468(3)	1.6463(4)	1.6463(3)	1.6471(5)
X–O	1.8867(3)	1.8928(5)	1.9003(5)	1.9033(6)	1.9256(2)	1.9267(4)	1.9711(4)	2.0188(5)
Z–O	2.1944(3)	2.2228(5)	2.2406(5)	2.2555(6)	2.3233(3)	2.3234(5)	2.3436(4)	2.3615(5)
Z–O	2.3424(3)	2.3744(5)	2.3946(5)	2.4178(6)	2.4882(3)	2.4875(5)	2.4970(4)	2.5029(5)
				Anharmonic refinement				
O								
x	0.03322(8)	0.0343(1)	0.0349(1)	0.0357(1)	0.03820(8)	0.0384(1)	0.03911(7)	0.0394(1)
y	0.05004(8)	0.0489(1)	0.0484(1)	0.0474(1)	0.04531(8)	0.0453(1)	0.04667(7)	0.0485(1)
z	0.65341(8)	0.6531(1)	0.6530(1)	0.6528(1)	0.65142(7)	0.6515(1)	0.65330(6)	0.6553(1)
B								
O	0.436	0.453	0.442	0.499	0.481	0.378	0.445	0.371
T	0.298	0.287	0.299	0.357	0.281	0.288	0.327	0.390
X	0.329	0.347	0.209	0.333	0.421	0.289	0.262	0.347
Z	0.632	0.581	0.567	0.609	0.436	0.390	0.420	0.450
T–O	1.6308(9)	1.631(1)	1.635(2)	1.635(2)	1.6466(9)	1.645(1)	1.6439(8)	1.647(1)
X–O	1.8877(9)	1.896(1)	1.904(2)	1.909(2)	1.9269(9)	1.928(1)	1.9722(8)	2.019(1)
Z–O	2.200(1)	2.224(1)	2.240(2)	2.257(2)	2.3223(9)	2.324(1)	2.3448(8)	2.362(1)
Z–O	2.345(1)	2.376(1)	2.394(2)	2.418(2)	2.4873(9)	2.488(1)	2.4985(8)	2.503(2)

indicative of the d_{z^2} orbital. MnAG#1, with about one-third the amount of Fe compared with FAG, shows correspondingly lower peak heights. Each lobe is oriented toward the coordination cuboid's face consisting of edges shared with the neighboring *Z* and *X* (Al) polyhedra. Lobes from three Fe sites point toward the 16*b* site, which is the largest interstitial site in this structure, which seems to lead to a local deformation of this essentially low-electron-density region (Fig. 3). This dumbbell-shaped deformation cannot be seen in other compounds with garnet structure investigated so far.

As with previous cases of electron density deformation indicating aspherical electron density distribution of the static atom (1, 2, 12, 13), the deformation at the *Z* site disappears in the anharmonic refinement. The dumbbell at the 16*b* site, however, persists.[1]

[1]See NAPS document No. 05493 for 94 pages of supplementary material. This is not a multi-article document. Order from NAPS c/o Microfiche Publications, P.O. Box 3513, Grand Central Station, New York, NY 10163-3513. Remit in advance in U.S. funds only $52.00 for photocopies or $6.00 for microfiche. There is a $25.00 invoicing charge on all orders filled before payment. Outside U.S. and Canada add postage of $4.50 for the first 20 pages and $1.00 for each 10 pages of material thereafter, or $5.00 for the first microfiche and $1.00 for each microfiche thereafter.

The 48*g* site shows peaks of 0.9 e/Å^3 height in MnAG#1, 0.5 e/Å height in FAG, 0.3–0.4 e/Å^3 height in CAG, and 0.2 e/Å^3 height in MnAG#2, with no positive peak detected in MgAG or CFG. The existence of positive residuals at this site has been attributed to interference between diffracted rays from domains with differently oriented crystallographic motifs (1). When these two garnet motifs sharing a common lattice (corresponding to a common *X* site arrangement) are viewed from the origin and crystallographic axes for one orientation, the alternate orientation has the *T*, *Z*, and oxygen sites shifted to positions corresponding to an alternative permutation of axes. The position of the *X* site remains invariant, whereas the *T* and *Z* sites appear to be shifted to the 48*g* site, and oxygen at the general position becomes situated at (*y*, *x*, *z*) versus (*x*, *y*, *z*) for the original orientation. Thus, the atomic arrangement becomes that pertaining to an opposite-handed choice of axes, but again, when viewed from a common origin and set of axes. This is *not* to say that this structure is enantiomorphic (it is not). This orientation can be found in the original motif if the origin is shifted to (1/4, 1/4, 1/4), so the garnet structure actually contains atomic arrangements

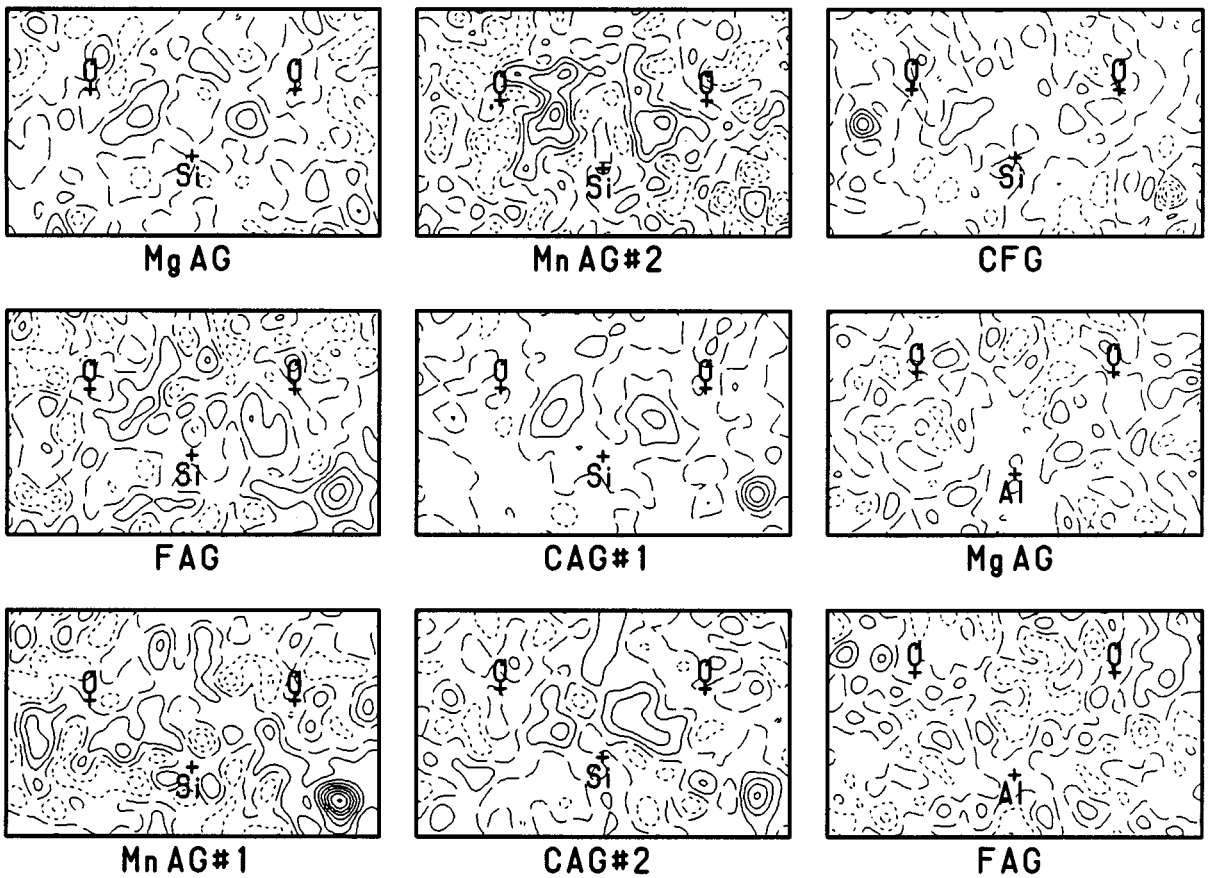

FIG. 2. Difference Fourier sections for the harmonic refinement along the O–*T*–O plane for the seven crystals and the O–*X*–O plane for MgAG and FAG. The 48*g* site is also approximately on the O–*T*–O plane near the lower right corner of the section. Map dimension is 3×5 Å. Positive contours are shown in full lines, zero contours in broken lines, and negative contours in dotted lines with increment 0.1 e/Å .

corresponding to both motif orientations. Thus, "*d*-glide twinning" and "twinning along the (110) planes" (Ref. (1)) are equivalent in this particular case, though the latter seems to be a better expression describing the situation suggested to be occurring in the atomic arrangement of the two motifs.

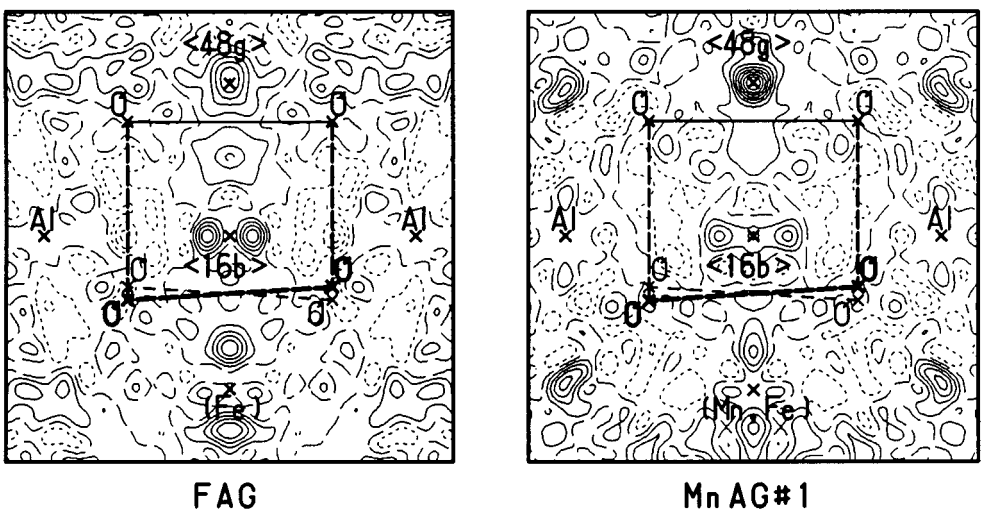

FIG. 3. Difference Fourier sections for the harmonic refinement of the two ferrogarnets along a plane passing through the *X* (Al), *Z* (with Fe^{2+}), 48*g*, and 16*b* sites, also showing the twisted triangular prismatic oxygen arrangement around the 16*b* position. The two upper oxygens are also approximately on the plane. Map dimension is 5×5 Å. Contours are plotted as in Fig. 2.

ACKNOWLEDGMENTS

All experimental measurements were made at the Department of Geosystem Sciences, Nihon University.

REFERENCES

1. H Sawada, *J. Solid State Chem.* **132,** 300 (1997).
2. H. Sawada, *J. Solid State Chem.* **132,** 432 (1997).
3. G. A. Novak and G. V. Gibbs, *Am. Mineral.* **56,** 791 (1971).
4. S. Sasaki, "KEK Internal," Vol. 87-3. National Laboratory for High Energy Physics, Tsukuba, 1987.
5. "International Tables for X-Ray Crystallography," Vol. IV. Kynoch Press, Birmingham, UK, 1974.
6. M. Tokonami, *Acta Crystallogr.* **19,** 486 (1965).
7. "International Tables for X-Ray Crystallography," Vol. III. Reidel, London, 1983.
8. W. F. Kuhs, *Acta Crystallogr., Sect. A* **40,** 133 (1984).
9. H. Sawada, *Mater. Res. Bull.* **32,** 873 (1997).
10. H. Sawada, *Mater. Res. Bull.* **31,** 355 (1996) [Erratum: H. Sawada, *Mater. Res. Bull.* **31,** 1045 (1996)].
11. H. Sawada, *Mater. Res. Bull.* **31,** 141 (1996).
12. H. Sawada, *J. Solid State Chem.* **134,** 182 (1997).
13. H. Sawada, *Mater. Res. Bull.* **31,** 361 (1996).
14. H. Sawada, *Mater. Res. Bull.* **29,** 127 (1994).
15. H. Sawada, *Mater. Res. Bull.* **30,** 341 (1995).